Eur. Phys. J. B **37**, 421–424 (2004)
DOI: 10.1140/epjb/e2004-00076-2

THE EUROPEAN PHYSICAL JOURNAL B

Comparison among the local atomic order of amorphous TM–Ti alloys (TM = Co, Ni, Cu) produced by mechanical alloying studied by EXAFS

K.D. Machado[a], J.C. de Lima, C.E.M. Campos, and T.A. Grandi

Departamento de Física, Universidade Federal de Santa Catarina, 88040-900 Florianópolis SC, Brazil

Received 12 October 2003
Published online 9 April 2004 –

Abstract. We have investigated the local atomic structure of amorphous TM–Ti alloys (TM = Co, Ni, Cu) produced by Mechanical Alloying by means of EXAFS analyses on TM and Ti K-edges. Coordination numbers and interatomic distances for the three alloys where found and compared. EXAFS results obtained indicated a shortening in the unlike pairs TM–Ti as the difference between d electrons of TM and Ti atoms increases, suggesting an increase in the chemical short range order (CSRO) from TM = Co to Cu.

PACS. 61.43.Dq Amorphous semiconductors, metals, and alloys – 61.10.Ht X-ray absorption spectroscopy: EXAFS, NEXAFS, XANES, etc. – 81.20.Ev Powder processing: powder metallurgy, compaction, sintering, mechanical alloying, and granulation

1 Introduction

Mechanical alloying (MA) technique [1] is an efficient method for synthesizing crystalline [2–5] and amorphous [6–10] materials, as well as stable and metastable solid solutions [11,12]. MA has also been used to produce materials with nanometer sized grains and alloys whose components have large differences in their melting temperatures and are thus difficult to produce using techniques based on melting. It is a dry milling process in which a metallic or non-metallic powder mixture is actively deformed in a controlled atmosphere under a highly energetic ball charge. The few thermodynamics restrictions on the alloy composition open up a wide range of possibilities for property combinations [13], even for immiscible elements [14]. The temperatures reached in MA are very low, and thus this low temperature process reduces reaction kinetics, allowing the production of poorly crystallized or amorphous materials.

We have used MA to produce three amorphous TM–Ti alloys: $Co_{57}Ti_{43}$ (a-$Co_{57}Ti_{43}$), $Ni_{60}Ti_{40}$ (a-$Ni_{60}Ti_{40}$) and $Cu_{64}Ti_{36}$ (a-$Cu_{64}Ti_{36}$) starting from the crystalline elemental powders. In reference [6] a-$Co_{57}Ti_{43}$ was studied by EXAFS and X-ray diffraction. In reference [7] we found coordination numbers and interatomic distances for the first neighbors for a-$Ni_{60}Ti_{40}$ using EXAFS and RMC simulations [15–17] of its total structure factor $S(K)$. Here, we studied a-$Cu_{64}Ti_{36}$ by EXAFS, and coordination numbers and interatomic distances were found and compared to those found for the other alloys. Due to its selectivity and high sensitivity to the chemical environment around a specific type of atom of an alloy, EXAFS is a technique (good reviews are found in Refs. [18–21]) very suitable to investigate the local atomic order of crystalline compounds and amorphous alloys. Anomalous wide angle X-ray scattering (AWAXS) is also a selective technique, but due to the small $K_{\max}$ that can be achieved on Ti K-edge ($\sim$4 Å^{-1}), little information could be obtained from an AWAXS experiment at the Ti K-edge. On the other hand, EXAFS measurements performed on this edge extended up to $\sim$16 Å^{-1} in some alloys, allowing the determination of structural data with reasonable accuracy. Using this technique, we have determined coordination numbers and interatomic distances in the first coordination shell of a-$Cu_{64}Ti_{36}$. In addition, the chemical short range order (CSRO) in the three TM–Ti alloys were compared and it increases as TM goes from Co to Cu, in accordance with results reported by Hausleitner and Hafner using MD simulations [22].

2 Experimental procedure

Blended TM (TM = Co, Ni and Cu) and Ti crystalline elemental powders (Co:Vetec, 99.7%, particle size < 10 μm; Ni: Merck, 99.5%, particle size < 10 μm; Cu: Vetec 99.5%, particle size < 10 μm; Ti: BDH, 99.5%, particle size < 10 μm), with initial nominal compositions $TM_{60}Ti_{40}$, were sealed together with several steel balls, under an argon atmosphere, in a steel vial (more details can be seen at Refs. [6,7]). The ball-to-powder weight ratio was 5:1 for the four alloys. The vial was mounted in a Spex 8000 shaker mill and milled for 9 h. A forced ventilation system was used to keep the vial temperature

[a] e-mail: kleber@fisica.ufsc.br

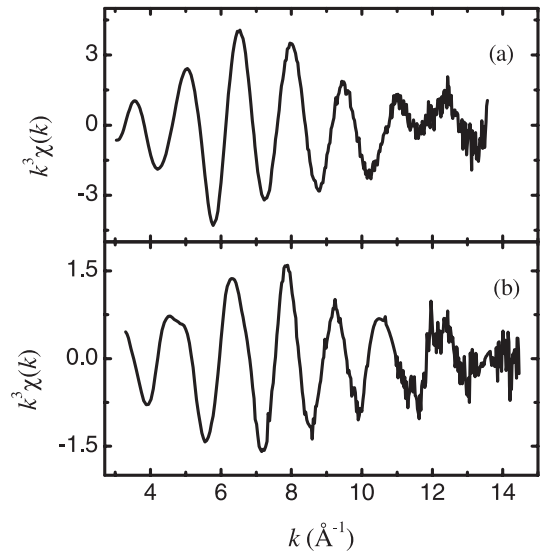

Fig. 1. Weighted experimental EXAFS spectra: (a) at the Cu K edge and (b) at the Ti K edge.

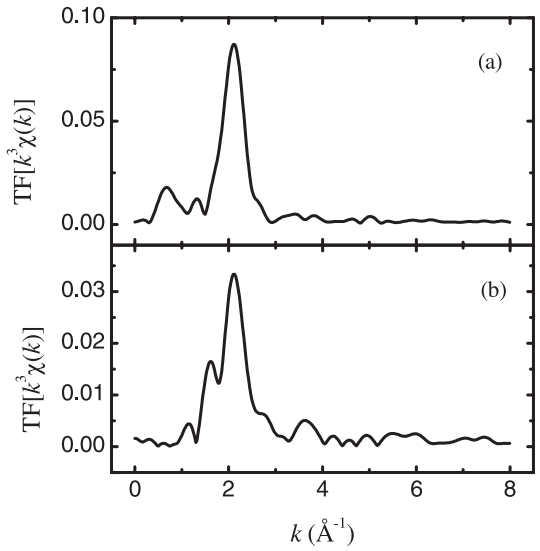

Fig. 2. Fourier transformation of experimental EXAFS spectra: (a) at the Cu K-edge and (b) at the Ti K-edge.

close to room temperature. The composition of the as-milled powder was measured using the Energy Dispersive Spectroscopy (EDS) technique, giving the compositions $Co_{57}Ti_{43}$, $Ni_{60}Ti_{40}$ and $Cu_{64}Ti_{36}$, and impurity traces were not observed. EXAFS measurements were carried out on the D04B beam line of LNLS (Campinas, Brazil), using a channel cut monochromator (Si 111), two ionization chambers as detectors and a 1 mm entrance slit. This yielded a resolution of about 1.6 eV at the Ti K edge and 3.9 eV at the Co, Ni and Cu K edges. All data were taken at room temperature in the transmission mode. The energy and average current of the storage ring were 1.37 GeV and 120 mA, respectively.

3 Results and discussion

The EXAFS oscillations $\chi(k)$ on Cu and Ti K edges of a-$Cu_{64}Ti_{36}$ are shown in Figure 1 weighted by k^3. After standard data reduction procedures using Winxas97 software [23], they were filtered by Fourier transforming $k^3\chi(k)$ on both edges (Cu edge, 3.25–13.6 Å^{-1} and Ti edge, 3.5–14.5 Å^{-1}) using a Hanning weighting function into r-space (Fig. 2) and transforming back the first coordination shells (1.30–2.67 Å for Co edge and 1.85–3.24 Å for Ti edge). Filtered spectra were then fit by using Gaussian distributions to represent the homopolar and heteropolar bonds [24]. We also used the third cumulant option of Winxas97 to investigate the presence of asymmetric shells. The amplitude and phase shifts relative to the homopolar and heteropolar bonds needed to fit them were obtained from ab initio calculations using the spherical waves method [25] and FEFF software.

Figure 3 shows the experimental and the fitting results for the Fourier-filtered first shells on Cu and Ti edges. Structural parameters extracted from the fits, including the errors in these values, are listed in Table 1. This table

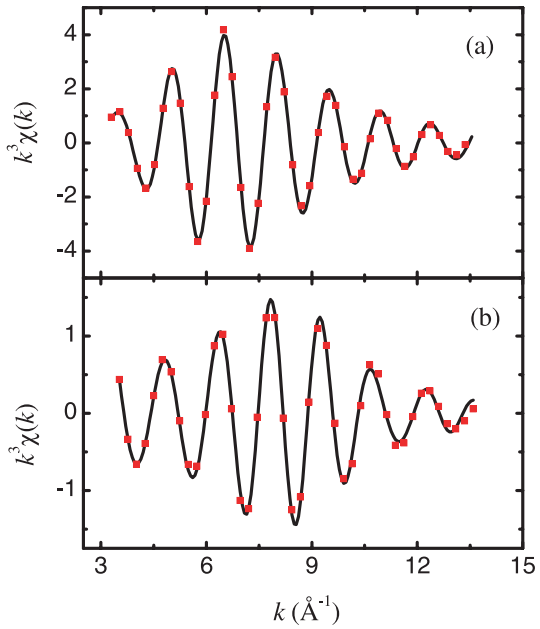

Fig. 3. Fourier-filtered first shell (full line) and its simulation (squares) for a-$Cu_{64}Ti_{36}$ at the (a) Cu K edge, (b) Ti K edge.

also shows data concerning crystalline Cu_2Ti (c-Cu_2Ti, JCPDS card No. 200371). It can be seen from Table 1 that the number of Cu–Cu pairs in a-$Cu_{64}Ti_{36}$ is much higher than it is in c-Cu_2Ti, whereas the Cu–Cu average interatomic distance increases in the amorphous alloy. There is a shortening in the Cu–Ti distance in a-$Cu_{64}Ti_{36}$, which becomes shorter that the Cu–Cu average distance, but the number of these pairs are almost the same. Concerning Ti–Ti pairs, there is a reduction both in its number and distance when compared to c-Cu_2Ti.

As it can be seen in Table 1, on the Cu edge, two Cu–Cu subshells and one Cu–Ti shell were considered in the first shell in order to find a good fit, whereas on the

Table 1. Structural data determined for a-$Cu_{64}Ti_{36}$. The numbers in parenthesis are the errors in the values.

EXAFS										
	Cu K-edge					Ti K-edge				
R factor	4.2					5.4				
Bond type	Cu–Cu[1]		Cu–Ti			Ti–Cu			Ti–Ti	
N	2.5 (0.4)	7.0 (1.0)	4.4 (0.6)			7.8 (1.0)			2.8 (0.4)	
r (Å)	2.31 (0.02)	2.80 (0.01)	2.42 (0.02)			2.42 (0.02)			2.70 (0.01)	
σ^2 (Å$\times 10^{-2}$)	0.925 (0.1)	2.51 (0.2)	3.47 (0.4)			3.47 (0.4)			1.01 (0.1)	
c-Cu_2Ti										
Bond type	Cu–Cu[2]			Cu–Ti[3]			Ti–Cu[4]			Ti–Ti[5]
N	2	2	2	2	1	4	4	2	2	2
r (Å)	2.54	2.58	2.58	2.61	2.63	2.58	2.61	2.63	2.93	3.32

[1]There are 9.5 pairs at $\langle r\rangle = 2.67$ Å. [2]There are 4 pairs at $\langle r\rangle = 2.56$ Å. [3]There are 5 pairs at $\langle r\rangle = 2.60$ Å. [4]There are 10 pairs at $\langle r\rangle = 2.60$ Å. [5]There are 4 pairs at $\langle r\rangle = 3.08$ Å.

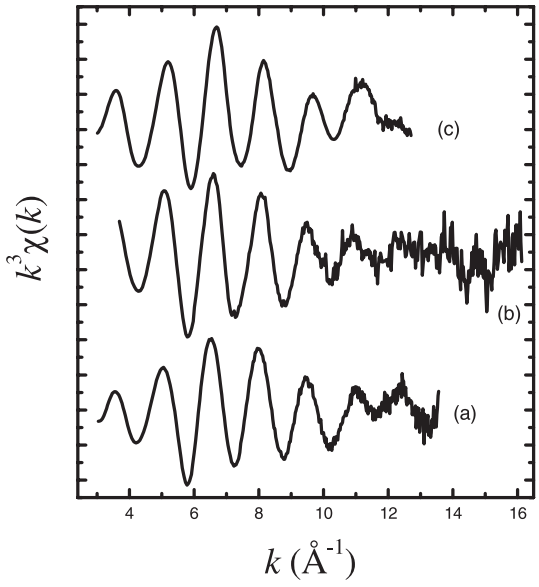

Fig. 4. Weighted EXAFS oscillations $k^3\chi(k)$ on the TM K edge for (a) a-$Cu_{64}Ti_{36}$, (b) a-$Ni_{60}Ti_{40}$ and (c) a-$Co_{57}Ti_{43}$.

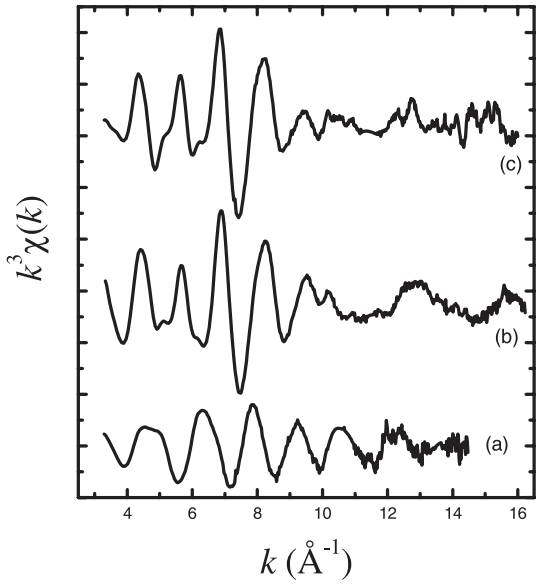

Fig. 5. Weighted EXAFS oscillations $k^3\chi(k)$ on the Ti K edge for (a) a-$Cu_{64}Ti_{36}$, (b) a-$Ni_{60}Ti_{40}$ and (c) a-$Co_{57}Ti_{43}$.

Ti edge one shell of Ti–Cu and one shell of Ti–Ti were needed. We started the fitting procedure using one shell for all pairs. This choice did not produce a good quality fit of Fourier-filtered first shells on the Cu edge. Besides that, the well-known relations below were not verified in fitting EXAFS data:

$$c_i N_{ij} = c_j N_{ij}$$
$$r_{ij} = r_{ji}$$
$$\sigma_{ij} = \sigma_{ji}$$

where c_i is the concentration of atoms of type i, N_{ij} is the number of j atoms located at a distance r_{ij} around an i atom and σ_{ij} is the half-width of the Gaussian. By considering two Cu–Cu sub-shells the quality of the fit on the Cu edge was much improved (see Fig. 3). Moreover, the relations above were satisfied.

It is interesting now to compare EXAFS data found for the three alloys. Figure 4 shows the weighted EXAFS oscillations $k^3\chi(k)$ obtained on the TM K edges of the three TM–Ti alloys. The oscillations on the three K edges are very similar, with small differences in the amplitudes of the oscillations.

Figure 5 shows the three weighted EXAFS oscillations $k^3\chi(k)$ on the Ti K edges. $k^3\chi_{\rm Ti}(k)$ for a-$Co_{57}Ti_{43}$ and a-$Ni_{60}Ti_{40}$ are very similar, indicating that Ti atoms are found in similar chemical environments. However, $k^3\chi_{\rm Ti}(k)$ for a-$Cu_{64}Ti_{36}$ shows a different behavior, which reflects the differences found in the coordination number determined for Ti atoms in this alloy. For a better comparison, structural data found for the other alloys are listed in Table 2.

From Tables 1 and 2, it can be seen that the number of TM-TM pairs increases from TM = Co to Cu, and the

Table 2. Structural data found for amorphous TM–Ti alloys (average values). The numbers in parenthesis are the errors in the values.

	a-$Co_{57}Ti_{43}$ [6]			
	Co K-edge		Ti K-edge	
R factor	1.9		2.9	
Bond type	Co–Co	Co–Ti	Ti–Co	Ti–Ti
N	6.0 (0.8)	6.0 (0.8)	7.9 (1.0)	4.9 (0.7)
r (Å)	2.50 (0.01)	2.52 (0.01)	2.52 (0.01)	2.98 (0.02)
σ^2 (Å$\times 10^{-2}$)	1.45 (0.2)	4.57 (0.6)	4.57 (0.6)	1.36 (0.1)
	a-$Ni_{60}Ti_{40}$ [7]			
	Ni K-edge		Ti K-edge	
R factor	1.5		3.5	
Bond type	Ni–Ni	Ni–Ti	Ti–Ni	Ti–Ti
N	8.8 (1.2)	5.2 (0.6)	7.9 (1.0)	5.5 (0.8)
r (Å)	2.58 (0.02)	2.55 (0.01)	2.55 (0.01)	2.93 (0.02)
σ^2 (Å$\times 10^{-2}$)	2.03 (0.3)	0.33 (0.04)	0.33 (0.04)	0.003 (0.0008)

same behavior is seen in the interatomic distances. Concerning Ti–Ti pairs, there is an increase in the number of these pairs from Co to Ni, but in a-$Cu_{64}Ti_{36}$ it decreases by almost 3 atoms, indicating a different chemical environment around Ti atoms in this alloy. This fact is reinforced if Ti–Ti interatomic distances are considered. There is a small reduction in the distance from Co to Ni and a very large reduction from Ni to Cu. It should be noted that the average Cu–Cu interatomic distance found by EXAFS analysis is larger than that for Cu–Ti pairs. This is an important feature, and it is also seen in a-$Ni_{60}Ti_{40}$. In fact, considering TM–Ti pairs, it can be seen that their interatomic distances decrease with the TM atomic number. The number of TM–Ti pairs also lowers when TM goes from Co to Cu. According to Hausleitner and Hafner [22], for TM–Ti alloys this shortening in the TM–Ti interatomic distance is associated with a change of the d-band electronic density of states in the TM–Ti alloys from a common-band to a split-band form, which depends on the difference of d-electrons in the TM and Ti atoms. Since this difference increases from Co to Cu, we should expect that the shortening effect would be weaker in a-$Co_{57}Ti_{43}$, increasing for a-$Ni_{60}Ti_{40}$ and reaching its maximum value in a-$Cu_{64}Ti_{36}$, and this is verified in our results. Fukunaga et al. also found this shortening in a-$Ni_{40}Ti_{60}$ produced by MQ [26]. It is important to note that this shortening effect was also confirmed by RMC simulations [15–17] in a-$Ni_{60}Ti_{40}$ [7] and a-$Cu_{64}Ti_{36}$ (results to be published elsewhere). This reduction in the TM–Ti interatomic distance indicates that the CSRO in TM–Ti alloys increases from Co–Ti to Cu–Ti alloys.

4 Conclusion

An amorphous $Cu_{64}Ti_{36}$ alloy was produced by Mechanical Alloying technique and its local atomic structure was determined from EXAFS analysis. We could find coordination numbers and interatomic distances for the first neighbors of this alloy. The results obtained were compared to those found in c-Cu_2Ti and also with those determined for other two TM–Ti alloys (TM = Co and Ni) produced by MA. The most important feature considering these alloys is the decrease in TM–Ti interatomic distance as a function of the TM atomic number, as proposed by Hausleitner and Hafner [22] to TM–Ti alloys. This effect can be associated to the CSRO in the alloys, which increases from Co to Cu.

We thank the Brazilian agencies CNPq, CAPES and FINEP for financial support. We also thank LNLS staff for help during measurements (proposal Nos. XAS 799/01 and XAS 998/01). This study was partially supported by LNLS.

References

1. C. Suryanarayana, Prog. Mater. Sci. **46**, 1 (2001)
2. K.D. Machado, J.C. de Lima, C.E.M. Campos, T. Grandi, A.A.M. Gasperini, Sol. State Commun. **127**, 477 (2003)
3. C.E.M. Campos, J.C. de Lima, T.A. Grandi, K.D. Machado, P.S. Pizani, Sol. State Commun. **123**, 179 (2002)
4. C.E.M. Campos, J.C. de Lima, T.A. Grandi, K.D. Machado, P.S. Pizani, Physica B **324**, 409 (2002)
5. J.C.D. Lima, E.C. Borba, C. Paduani, V.H.F. dos Santos, T.A. Grandi, H.R. Rechenberg, I. Denicoló, M. Elmassalami, A.P. Barbosa, J. Alloys Comp. **234**, 43 (1996)
6. K.D. Machado, J.C. de Lima, C.E.M. de Campos, T.A. Grandi, A.A.M. Gasperini, Sol. State Commun. (submitted to publication)
7. K.D. Machado, J.C. de Lima, C.E.M. de Campos, T.A. Grandi, D.M. Trichês, Phys. Rev. B **66**, 094205 (2002)
8. J.C.D. Lima, D.M. Trichês, T.A. Grandi, R.S. de Biasi, J. Non-Cryst. Solids **304**, 174 (2002)
9. A.W. Weeber, H. Bakker, Physica B **153**, 93 (1988)
10. C.E.M. Campos, J.C. de Lima, T. Grandi, K. Machado, P. Pizani, Sol. State Commun. **126**, 611 (2003)
11. D.K. Mukhopadhyay, C. Suryanarayana, F.H. Froes, Scripta Metall. Mater. **30**, 133 (1994)
12. A.R. Yavari, P.J. Desré, T. Benameur, Phys. Rev. Lett. **68**, 2235 (1992)
13. J.M. Poole, J.J. Fischer, Mater. Technol. **9**, 21 (1994)
14. M. Abbate, W.H. Schreiner, T.A. Grandi, J.C. de Lima, J. Phys.: Condens. Matter **13**, 5723 (2001)
15. R.L. McGreevy, L. Pusztai, Mol. Simul. **1**, 359 (1988)
16. RMCA version 3, R.L. McGreevy, M.A. Howe, J.D. Wicks, 1993, available at `http://www.studsvik.uu.se`
17. R.L. McGreevy, J. Phys.: Condens. Matter **13**, 877 (2001)
18. P.A. Lee, P. Citrin, P. Eisenberger, B. Kincaid, Rev. Mod. Phys. **53**, 769 (1981)
19. B.K. Teo, D.C. Joy, *EXAFS Spectroscopy, Techniques and Applications* (Plenum, New York, 1981)
20. T.M. Hayes, J.B. Boyce, *Solid State Physics* (Academic Press, New York, 1982), Vol. 37, p. 173
21. D.C. Koningsberger, R. Prins, *X-ray Absorption* (Wiley, New York, 1988)
22. C. Hausleitner, J. Hafner, Phys. Rev. B **45**, 128 (1992)
23. T. Ressler, J. Phys. **7**, C2 (1997)
24. E.A. Stern, D.E. Sayers, F.W. Lytle, Phys. Rev. B **11**, 4836 (1975)
25. J.J. Rehr, J. Am. Chem. Soc. **113**, 5135 (1991)
26. T. Fukunaga, N. Watanabe, K. Suzuki, J. Non-Cryst. Solids **61-62**, 343 (1984)